Taylor & Francis
Taylor & Francis Group

Molecular Crystals and Liquid Crystals

ISSN: 1542-1406 (Print) 1563-5287 (Online) Journal homepage: http://www.tandfonline.com/loi/gmcl20

Judd-Ofelt analysis of Nd^{3+} doped phosphate glass: The effect of Ba/Sr ratio

Vadim O. Kozhanov, Alexander N. Zaderko, Olga Yu. Boldyrieva & Vladyslav V. Lisnyak

To cite this article: Vadim O. Kozhanov, Alexander N. Zaderko, Olga Yu. Boldyrieva & Vladyslav V. Lisnyak (2016) Judd-Ofelt analysis of Nd^{3+} doped phosphate glass: The effect of Ba/Sr ratio, Molecular Crystals and Liquid Crystals, 639:1, 78-86, DOI: 10.1080/15421406.2016.1254554

To link to this article: http://dx.doi.org/10.1080/15421406.2016.1254554

MOLECULAR CRYSTALS AND LIQUID CRYSTALS
2016, VOL. 639, 78–86
http://dx.doi.org/10.1080/15421406.2016.1254554

Taylor & Francis
Taylor & Francis Group

Judd-Ofelt analysis of Nd^{3+} doped phosphate glass: The effect of Ba/Sr ratio

Vadim O. Kozhanov, Alexander N. Zaderko, Olga Yu. Boldyrieva, and Vladyslav V. Lisnyak

Faculty of Chemistry, Taras Shevchenko National University of Kyiv, Kyiv, Ukraine

ABSTRACT

Here we disclosed the substantial effect of the local medium in the vicinity of the excited Nd^{3+} ions on the optical properties and the laser characteristics of glasses. The UV-Vis absorption of the laser BaO/SrO–P_2O_5–Al_2O_3–K_2O–B_2O_3–La_2O_3 glasses doped with Nd^{3+} ions is measured at 25 °C. Judd-Ofelt (JO) theoretical analysis of 4f electron transitions in the Nd^{3+} absorption spectra was performed. From the JO intensity parameters, a set of the laser $^4F_{3/2} \rightarrow {}^4I_{11/2}$ transitions characteristics are found and stimulated emission cross-sections are characterized. The effect of different Ba/Sr ratio on the structure-properties relationships in the glasses is shown.

KEYWORDS

Judd-Ofelt theory; Optical absorption; Rare earth ions in glasses; Neodymium laser characteristics

1. Introduction

This study relates to low-cost fiber lasers that operated at the high power single-mode setting and formed from the rare earth (RE) glass. In the infrared optical amplification, much attention is given to the laser glasses doped with Nd^{3+}. Their potential application is related to the radiative efficiency of the $^4F_{3/2} \rightarrow {}^4I_{11/2}$ emission found at around 1.06 μm [1]. For the miniature solid-state lasers, one requires a glassy medium with a high concentration of activator ions, up to 13 mass%. It is not a surprise that the optical properties and the laser characteristics observed for Nd^{3+} depends on the used glass, its composition, and microstructure. On the other hand, one can apply a mixture of RE^{3+} and Nd^{3+} instead of the single Nd^{3+} activator [2] to reduce the optical density improving optical measurements. The doped phosphate glasses, e.g. containing isomorphic La^{3+} and Nd^{3+} combinations in which lanthanum is a diluting agent, are ideal for such purpose.

It is well known that the spectroscopic parameters of the trivalent RE ions depend remarkably on the chemical composition of the glass matrix. The composition determines the structure and the nature of the bonds [3, 4]. The laser glasses within the alumina-borate-phosphates (ABP) family prove the high optical homogeneity and isotropy. A lot of them show the laser excitation with up to 100% efficiency and the high luminescence quantum yield [5]. Totally, the representatives of ABP glasses combine reasonable transparency and the highest peak output power [6]. Their valuable properties might be optimized that holds promise to reduce the luminescence decay time without the losses in the laser power.

CONTACT V. O. Kozhanov kozhanov1994512@gmail.com; Dr. V. V. Lisnyak lisnyak@univ.kiev.ua Faculty of Chemistry, Taras Shevchenko National University of Kyiv, 64, Volodymyrska Str., 01060 Kyiv, Ukraine.
Color versions of one or more of the figures in the article can be found online at www.tandfonline.com/gmcl.

Earlier, in [7], we reported on the f–f transitions in Nd^{3+} ions that doped BaO/SrO–P_2O_5–Al_2O_3–K_2O–B_2O_3–La_2O_3 glasses. Using the Judd-Ofelt (JO) theory [8], we can estimate the probability of f–f transitions and the branching ratios basing on an analysis of optical absorption spectra [9, 10]. The theoretical assessment could be done for strong bands which peaks positioned at ca. 805, 744, 684, 583, 525, 428, and 355 nm. Changes in the composition of the glassy media have often drastically effected on the environment of Nd^{3+} [11]. So, the electronic transitions within the 4f shell could be sensitive to them. Surprisingly, the changes may correlate with the variations in the rigidity of medium estimated against the glass composition, e.g. with Ba/Sr ratio. All the above led us to undertake a new estimation of the laser glasses parameters on the basis of JO theory and Sakka-Dimitrov (SD) approach [12].

2. Experimental

2.1. Glass preparation

The prototype glass having a composition of mass% (58.0) P_2O_5, (12.0) BaO, (13.0) K_2O, (2.0) SiO_2, (8.0) Al_2O_3, (4.0) B_2O_3, (0.5) Nd_2O_3, (2.5) La_2O_3 was selected for this study. The components for the glassmaking were reagent grade $Ba(NO_3)_2$, $Sr(NO_3)_2$, $(NH_4)_2HPO_4$, KH_2PO_4, SiO_2, La_2O_3, and Nd_2O_3. These reagents were additional purified from coloring impurities as in [7]. To obtain SrABP and mixed Ba/SrABP glasses, the substitution of Ba for Sr was conducted remaining the constant molar fraction of the alkaline earth oxide in the glass. The ratio of Ba to Sr in the glass changes within the molar fraction (x) increment of 0.25.

The mixtures of 20 g of the components, taken in the preset proportion, were thoroughly mixed before transfer to quartz crucibles, and then fused at above 1300 °C. Resulted melts were cast and obtained glasses are annealed in an automatic resistant oven. A series of ABP glasses with Ba that substituted for Sr were prepared and assigned as (molar ratio of Ba/Sr is shown in parentheses) BaABP (Ba/Sr = 1.0/0.0), Ba/SrABP1 (Ba/Sr = 0.75/0.25), Ba/SrABP2 (Ba/Sr = 0.50/0.50), Ba/SrABP3 (Ba/Sr = 0.25/0.75), and SrABP (Ba/Sr = 0.0/1.0).

2.2. Judd-Ofelt analysis

The annealed as-cast glass samples were cut into thin plates of typical size 10 × 10 × 2 mm and polished for future studies. Optical absorption spectra in the ultraviolet and visible (UV-VIS) regions were measured at room temperature by means of Shimadzu UV-2700 spectrophotometer, with 1 nm scan-rate. The JO intensity parameters, namely: Ω_2, Ω_4, and Ω_6, which are dependent on the local surrounding of Nd^{3+}, have been determined by a least-square fit of the calculated ($S_{calc.}$) to the measured ($S_{meas.}$) electric-dipole line strength. Both of them were found using the following formulas

$$S_{meas.} = \frac{3ch(2J+1)}{8\pi^3\bar{e}^2N}n\left(\frac{3}{n^2+2}\right)^2\int\frac{\alpha(\lambda)}{\lambda}d\lambda, \quad (1)$$

where N is the concentration of Nd^{3+} (cm^{-3}), h is the Planck's constant, n is the refractiveindex of studied medium (~1.52), ē is the charge of electron, c is the speed of light *in vacuum*, $\alpha(\lambda)$ is the absorption coefficient at the wavelength λ, which is determined from UV-VIS absorption measurements and equals $2.303D\times d^{-1}$, where D is the optical density, d is the absorption

layer thickness (ca. 2 mm),

$$S_{\text{calc.}} = \sum_{\lambda} \Omega_{\lambda} \left\langle (S, L)\, J \left\| U^{\lambda} \right\| \left(S', L'\right) J' \right\rangle, \tag{2}$$

where Ω_t are the JO intensity parameters, S, L, J and S', L', J' are the quantum numbers of respective terms, and $\langle \| U^{\lambda} \| \rangle$ is the doubly reduced matrix elements calculated in the intermediate coupling approximation [8,10].

Spontaneous emission probability ($A(J - J')$) is taken from

$$A(J - J') = \frac{64\pi^4 \bar{e}^2}{3h(2J+1)\bar{\lambda}^3} \frac{n(n^2+2)^2}{9} S_{\text{calc.}}(J - J'), \tag{3}$$

where $\bar{\lambda}$ is the mean wavelength of the absorption band.

The accuracy of the model predictions was evaluated by the mean squared deviation,

$$\delta = (S_{\text{calc.}} - S_{\text{meas.}})^2 / N, \tag{4}$$

where N is the number of lines what equals 7.

The radiative lifetime (τ_r) and the luminescence branching ratio ($\beta(J - J')$) are found from the respective Judd's parameters through the following equations:

$$\tau_r = \frac{1}{\sum A(J - J')}, \tag{5}$$

$$\beta(J - J') = \frac{(J - J')}{\sum A(J - J')}, \tag{6}$$

The stimulated emission cross-section (σ_{em}) is calculated as

$$\sigma_{\text{em}} = \frac{\lambda^4 \beta}{8\pi n_0^2 c \tau_r \Delta\lambda}, \tag{7}$$

where $\Delta\lambda$ is the full width at half maximum normalized on [6].

2.2. Empirical estimation of glasses properties

The glasses properties were estimated within the relations of SD, for details refer to [7]. Principally, such simulations bind the empirical equations with the component ratio dependence [12]. To calculate the average molar refraction (R_m) from the additive approach, we took the molar polarization ability of metal cations and oxygen anions from Shannon's work [13]. To estimate the ionic packing ratio (V_p), the same principle within the rigid sphere model was used. The optical basicity (Λ_{th}), the polarizability of oxygen ions ($\alpha(O^{2-})$) and the Goldhammer-Herzfeld (GH) criterion for metallization are calculated as in [14, 15].

The empirical optical parameters correspond to the respective electron and charge characteristics of a glass media as follows. The interaction of UV-Vis radiation and a matter, the ability of glass to create dipoles through a host matrix, is characterized by the value of R_m. Besides, the mobility of the electron cloud of oxygen ions can be estimated from the value of $\alpha(O^{2-})$. The electron-donor ability of oxygen ions in a glass matrix is deduced from Λ_{th}.

The molar volume of glasses (V_m) was found from the formula

$$V_m = \sum \frac{M_i X_i}{\rho}, \tag{8}$$

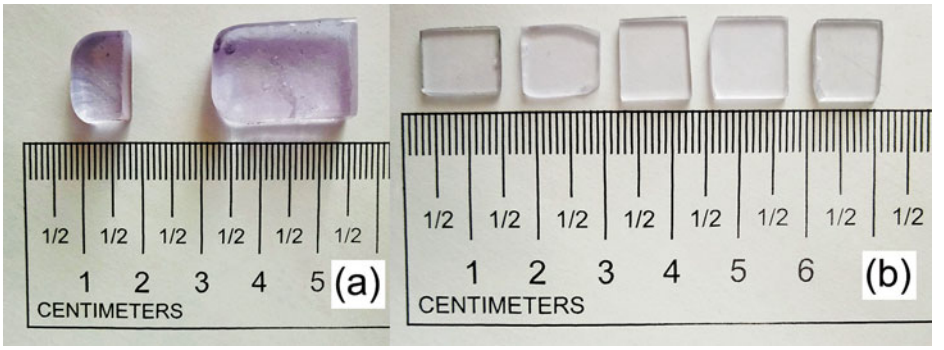

Figure 1. Photograph of as-cast glasses (a) and polished glass plates (b), from left to right: (a) SrABP and BaABP; (b) BaABP, Ba/SrABP1, Ba/SrABP2, Ba/SrABP3, and SrABP.

where ρ is the density of the glass sample measured gravimetrically, M_i and X_i are the molar mass and fraction, respectively, and the subscript i refers to the constituent oxides.

3. Results and discussion

Figure 1a display as-cast glasses samples that have good transparency.

In the absorption experiments, we used polished plates depicted in Fig. 1b. The UV-Vis absorption spectra of the studied glasses are shown in Fig. 2.

In Table 1 is summarized the parameters Ω_t those are determined from the values of $S_{\text{meas.}}$ for the intensive spectral lines (Fig. 2).

From the presented Ω_2, Ω_6 and Ω_4/Ω_6 parameters, it is obvious that there is an extreme trend toward the ratio of Ba to Sr. Definitely, the substitution of Ba^{2+} for Sr^{2+} affects considerably on the structure and properties of the initial BaABP matrix. It is also notable that the numerical values of δ are low in the comparison with the values of $S_{\text{meas.}}$ and $S_{\text{calc.}}$. The values of δ are acceptable for the Judd-Ofelt approximation for this glass matrix and each of them shows a good spectrum fit. The parameter Ω_2 can be considered as the criterion of ionicity/covalency of RE–O bonds. In other words, the value of Ω_2 depends on the symmetry

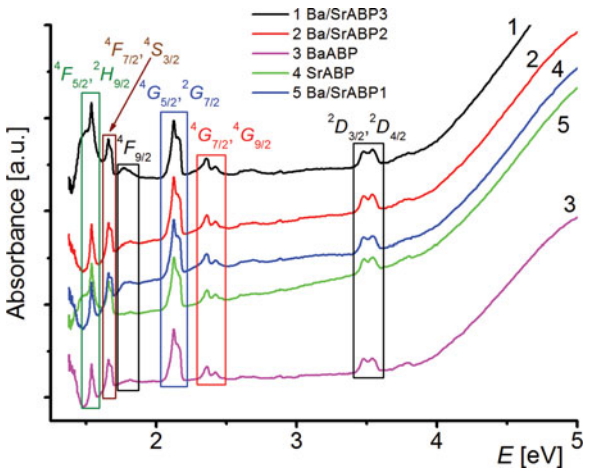

Figure 2. UV-Vis absorption spectra of ABP glasses. The final states of the transitions are labeled. The spectra are normalized by the plate thickness.

Table 1. The values of Judd-Ofelt parameters (Ω_t) and mean squared deviation (δ).

Glass	Ω_t, $\times 10^{-20}$ cm^2			Ω_4/Ω_6	δ, $\times 10^{-20}$ nm $\times$ cm^2
	Ω_2	Ω_4	Ω_6		
BaABP	3.73 ± 0.17	2.48 ± 0.20	3.33 ± 0.15	0.74	0.17
Ba/SrABP1	4.09 ± 0.17	2.58 ± 0.20	3.70 ± 0.15	0.70	0.61
Ba/SrABP2	4.72 ± 0.16	3.49 ± 0.19	3.90 ± 0.14	0.89	0.06
Ba/SrABP3	4.56 ± 0.49	3.57 ± 0.36	3.50 ± 0.90	0.90	0.08
SrABP	4.84 ± 0.35	2.87 ± 0.26	3.95 ± 0.73	0.73	0.40

of NdO_8 polyhedra. So, the highest symmetry of the surrounding of Nd^{3+} ion causes the lowest value of Ω_2 parameter that also corresponds to the highest ionicity of the Nd–O bonds. Besides, the parameter Ω_6 could be considered as a measure of the stiffness of an optic glass matrix. The Ba/SrABP2 glass shows the maximal stiffness and the highest asymmetry in the vicinity of the excited Nd^{3+} ions [16]. For the Ba/SrABP3 glass, the spectroscopic quality parameter, the ratio of Ω_4/Ω_6, has the highest value to foresee an efficient stimulated emission. It also can be an evidence of the highest intensity of the laser $^4F_{3/2} \rightarrow {}^4I_{11/2}$ transition. For the Ba/SrABP2 glass (Ba/Sr = 0.5/0.5), the covalence of Nd–O bonds is the highest (see Ω_2 in Table 1), probably, because of the most efficient Nd^{3+} coordination with the terminal oxygen of P = O sites. Thus, the increasing covalency of the Nd–O bonds causes the greater electron delocalization. In turn, the delocalization reduces the electron-electron pair interaction for the 4f shell. Finally, the lowering the energy of electron-electron transitions greatly increases the probability of the laser and pumping transitions [17, 18]. The values of $A(J - J')$, $\beta(J - J')$, τ_r, and σ_{em}, calculated by using Equations (3–7), are listed in Table 2.

The compositional dependence of the spontaneous emission probabilities of Nd^{3+}, $A(J - J')$, has observed for all ABP glasses. This is not a surprising situation since the values $A(J - J')$ are calculated using the intensity parameters Ω_t affected by the Nd^{3+} ions confinement. The magnitude of $A(J - J')$ for $J = 11/2$ and 13/2 increases monotonically, up to Ba/Sr = 0.25/0.75, with a decrease in the value of V_p which depends on the network modifier. Perhaps, the Ba ions have the special effect on $A(J - J')$. The substitution of Ba for Sr shows no if any influence on $\beta(J - J')$, but has a strong decreasing effect on τ_r. The complete substitution of Ba for Sr gives the controversial result (cf. respective data in Table 2). Surprisingly, the value of τ_r demonstrates a non-monotonic extreme dependence on the composition, in the range of Ba/Sr = 0.0–0.7/0.25. The reason of this is that, when the probability of the $^4F_{3/2} \rightarrow {}^4I_{13/2}$ transition increases with the content of Sr, at the same time, the glass density decreases. Therefore

Table 2. The spontaneous emission probabilities $A(J - J')$, luminescence branching ratio ($\beta(J - J')$), radiative lifetime (τ_r), stimulated emission cross-section (σ_{em}), and the ionic packing ratio (V_p) of prepared glasses.

Glass	$^4F_{3/2} \rightarrow {}^4I_J$, $\times 10^3$ s^{-1}						τ_r, ms	σ_{em}, $\times 10^{-20}$ cm^2	[a] V_p, %
	$J = 9/2$		$J = 11/2$		$J = 13/2$				
	$A(J - J')$	$\beta(J - J')$	$A(J - J')$	$\beta(J - J')$	$A(J - J')$	$\beta(J - J')$			
BaABP	693.5	0.38	930.0	0.51	185.2	0.10	0.55	3.8	68.9
Ba/SrABP1	734.3	0.37	1019.0	0.52	205.5	0.10	0.51	4.2	59.0
Ba/SrABP2	937.5	0.41	1135.0	0.50	217.0	0.09	0.44	4.7	50.1
Ba/SrABP3	955.9	0.41	1150.0	0.50	219.3	0.09	0.43	4.7	49.0
SrABP	807.9	0.38	1096.5	0.52	219.3	0.10	0.47	4.5	49.6

[a] V_p calculated at coordination numbers $CN_{Ba-O} = 8$ and $CN_{Sr-O} = 6$.

the resulted glass networks have a reduced ability to relax. Besides, the outcomes of our studies suggest that the Nd^{3+} and La^{3+} break some of the P–O–P bonds and occupy the definite network sites. This dual incorporation in the phosphate glass is shown to result in a dispersion of the Nd^{3+} ions. Because of this, the nearest Nd–Nd distances in the glass networks tend to elongate. From the laser efficiency perspective, such dilution of Nd^{3+} with La^{3+} prevents the concentration quenching of luminescence in the ABP glasses. We will notice that the average oxygen coordination number (CN) around the La^{3+} is expected to be from 6 to 7 for the metaphosphate glasses. And, nevertheless, it may take the value of 8 as for Ba metaphosphate glasses [19].

As seen from the Table 2, the values of τ_r are better for Ba/SrABP2 and Ba/SrABP3 glasses. Surprisingly, the values of σ_{em} for our glasses exceeding that of the reference material [11], which is recalculated to be σ_{em} ~3.8. This fact discloses the high potential of the initial reagents purification [4] and the cations substitution for the improvement of the laser parameters. To illustrate the effect of substitution, the experimental and empirical parameters are plotted, for a comparison, against the ratio of alkaline earth metals (Ba/Sr) in glasses, see Fig. 3.

If consider depicted correlations we can assume that the values of Λ_{th}, R_m, V_m, ρ, GH, and $\alpha(O^{2-})$ decrease smoothly from BaABP to SrABP glass, Fig. 3a. The parameters V_m and GH calculated from the additivity law show a similar increasing tendency as functions of Ba/Sr ratio. It is not a surprising situation, since all the parameters, V_m and GH, and also ρ, are

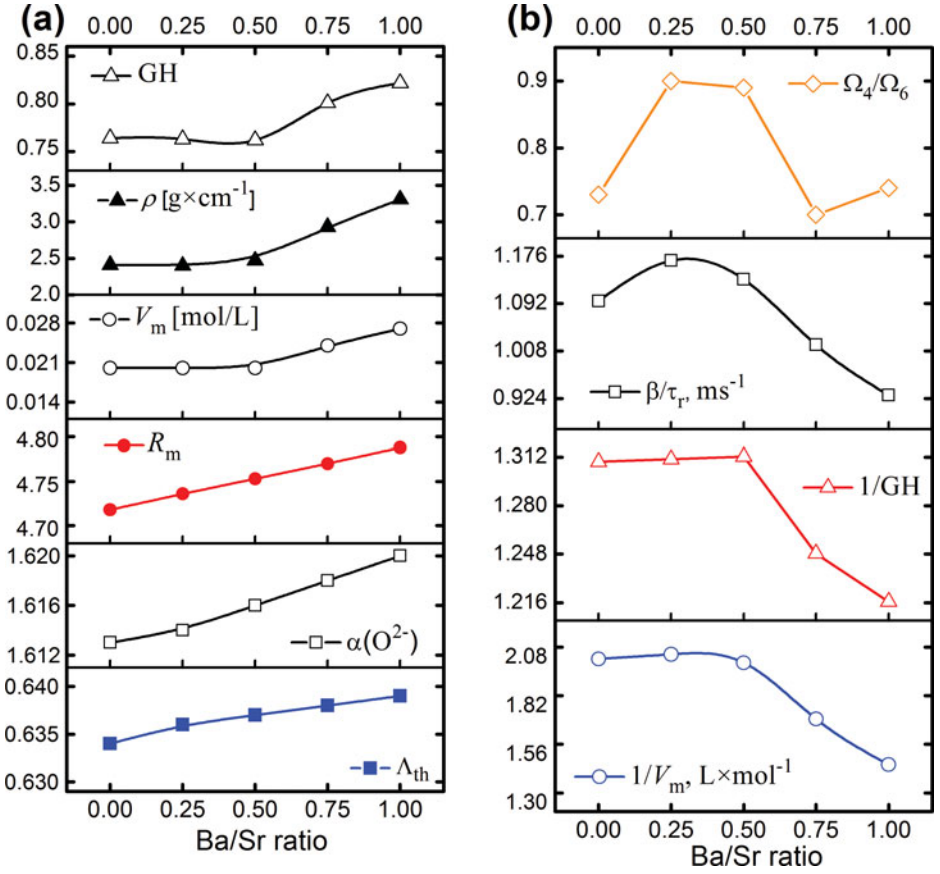

Figure 3. (a-b) Experimental and empirical parameters as functions of Ba/Sr ratio.

dependent on the molar masses of components. Naturally, this is due to the higher molar mass of Ba as compared with that of Sr.

In contrast to previously disclosed concentration behavior, another monotonic trend is apparent for the values of Λ_{th}, R_m and $\alpha(O^{2-})$. This fact can be described in the following way. It is clear that the contribution of two alkaline earth metals is only subjected to the change. Therefore, the induced variations in the optical parameters are isobathic and correlate with each of the alkaline earth metal contributions.

The simultaneous decrease in the reciprocal magnitudes (1/GH and $1/V_m$) is seen from Fig. 3b. To illustrate the relationship between G and 1/GH, below we will focus on their physical nature and consider the facts. As far as the GH criterion is a measure of the bond metallicity, the near-zero values of GH correspond to the metallic conductivity, while the GH→1 corresponds to the dielectric state. The half substitution of Ba by Sr decreases the GH values of the glass matrix, from 0.82 to 0.76. In this case, the increase of the metallicity is accompanied by a decrease in the electron-nuclei binding. Definitely, the value of 1/GH can be used to estimate the possibility of the electronic transitions between the levels of the partially filled 4f shell of Nd^{3+}. The latter can be explained by the less electron-nuclei interaction (ENI) and the more charge detrapping effect. The replacing of the more for the less electropositive alkaline earth metal ions lead to the more reliable electron transitions. This is the reason for a correlation between the spectroscopic parameters of the optic quality of glass, e.g. Ω_2, Ω_4/Ω_6 and β/τ_r, and the GH criterion. So, the extreme of the GH dependence at Ba/Sr = 0.50/0.50 is could be due to the decrease of the density and the changes in the energy relaxation pathways.

It is interesting to compare the concentration dependencies for the reciprocal magnitudes and the Judd-Ofelt intensity (β/τ_r and Ω_4/Ω_6) parameters because they have essentially the same origin, see Fig. 3b. The β/τ_r parameter estimated for the $^4F_{3/2}\rightarrow{}^4I_{11/2}$ transition is generally accepted as the criteria for laser action. To improve the β/τ_r parameter the probability of transition can be increased. The later gives reducing the influence of the ENI, as shown above for 1/GH. Thus, using the 1/GH as a criterion which corresponds to the transitions probability, one can find the same dynamic variations as for the β/τ_r and Ω_4/Ω_6 that are determined by the Judd-Ofelt theory. Since the GH criterion is deduced from the V_m by the formula

$$GH = \left[1 - \left(\frac{R_m}{V_m}\right)\right], \tag{9}$$

it is not surprising that the concentration dependence for $1/V_m$ shows a similar non-linear trend.

In sum, the polarizability and the possibility of energy transfer in the glass media are the functions that depend crucially on the structure and the composition. They both have a considerable effect on the spectral optical characteristics. The 1/GH criterion includes the density of glass media indirectly through the molar volume (see Equations 8 and 9). Since the density and the average molar refraction are interrelated with the energy transfer and the polarizability, so, the value of 1/GH represents correlated dynamics.

The concentration dependence of Ω_4/Ω_6, the spectroscopic quality parameter, shows an extreme behavior (Fig. 3b). This fact could be disclosed if one accounts the effect of the local bonding alteration near the excited Nd^{3+} ions. From a crystal chemical point of view, the distortion in Nd^{3+}–O shell could be considered as follows. Typically, neodymium in oxide glasses maintains a rather uniform coordination sphere of approximately 7 or 8 non-bridging oxygens [20]. The average coordination site of Nd^{3+} keeps the same in the different alkaline/alkaline earth alumina borosilicate glasses [20]. In the metaphosphate glass, the Nd^{3+} tends to the 7-fold oxygen coordination [21]. We suppose that the same conservation of the

trivalent neodymium coordination with oxygen, as found in [20, 21], should be valid for the multicomponent metaphosphate glass considered here.

Apart from these coordination rules, the rigidity of the net is tuned within a range of Ba^{2+} to Sr^{2+} ratio, see V_p in Table 2. This regulation is undoubtedly observed when the glass network conversing from the initial Ba-containing to that of the mixed Ba/Sr. In fact, the cation replacement induces changes, the source of which are the spatial difference in the dimensions of the voids occupied with the larger Ba^{2+} and the smaller Sr^{2+} cations. The cations fitted into voids are irregularly coordinated by the oxygen. The average oxygen CN around Ba in the metaphosphate glasses varies from 8 to 11 [19, 22, 23]. As was shown in [19, 24], in similar and resembling glasses, Sr is coordinated with 6 to 7.5 oxygen atoms. The glass seems to be influenced by the ability of Ba ions to coordinate strongly with more oxygen even in the presence of Sr ions. That is why it is not surprising that the different coordination ability stimulates the concurrence for the positions in the vicinity of Nd^{3+}.

4. Concluding remarks

We have analyzed the JO parameters for the ABP glasses with the different Ba/Sr ratio and obtained a set of the laser ${}^4F_{3/2} \rightarrow {}^4I_{11/2}$ transition characteristics, including the stimulated emission cross-sections. In the presently analyzed glasses, the structural changes taking place around the excited Nd^{3+} ions induce the improvement of the glass optical properties. In the Ba/SrABP glass series, where Ba^{2+} are progressively replaced by Sr^{2+}, the Ba^{2+} ions may preferentially stay in the vicinity of Nd^{3+}, so that the bond covalency does not change abruptly. Such observations become possible due to the high sensitivity of Nd^{3+} absorption spectroscopy and the JO analysis designed for a soft isotropic matter.

The substitution shows that the BaABP glasses can be improved in the proposed way. In general, by changing the composition of these glasses, excellent glass characteristics can be reached. Through the glass systems, the spontaneous emission probabilities of ${}^4F_{3/2} \rightarrow {}^4I_J$ ($J = 9/2$, 11/2 and 13/2) transitions increase with an increase of V_p. The latter varies markedly with the type of network modifier. Considering the substantial effect of the local medium, in the vicinity of the excited Nd^{3+} ions, the striking effect of a mixture of alkaline-earth cations on the glasses characteristics is disclosed.

References

[1] Sola, D. et al., (2015). *Optic Express*, *23*, 26356–26368.
[2] Takebe, H., Nageno, Y., & Morinaga, K. (1995). *J. Am. Ceram. Soc.*, *78*, 1161–1168.
[3] Weber, M. J. (1990). *J. Non-Cryst. Solids*, *123*, 208–222.
[4] Jacobs, R. R., & Weber, M. J. (1976). *IEEE J. Quantum Electron.*, *12*, 102–111.
[5] Krupke, W. F. (1974). *IEEE J. Quantum Electron.*, *10*, 450–457.
[6] Sarkisov, P. D., Sigaev, V. N., Golubev, N. V., & Savinkov, V. I. (Inventors) (August 2011). The optical phosphate glass. Patent of Russian Federation No.2426701.
[7] Popov, A. S. et al., (2016). *Funct. Mater.*, *23*, 174–182.
[8] Judd, B. R. (1962). *Phys. Rev.*, *127*, 750–761.
[9] Walsh, B. M. et al., (2002). *J. Opt. Soc. Am. B*, *19*, 2893–2903.
[10] Walsh, B. M. (2006). In: *Advances in Spectroscopy for Lasers and Sensing*, Di Bartolo, B. & Forte, O. (Eds.), Chapter 21, Springer: Dordrecht, The Netherlands, 403.
[11] Nageno, Y., Takebe, H., & Morinaga, K. (1993). *J. Am. Ceram. Soc.*, *76*, 3081–3086.
[12] Dimitrov, I. V., & Sakka, S. (1996). *J. Appl. Phys.*, *79*, 1736–1740.
[13] Shannon, R. D., & Fischer, R. X., (2006). *Phys. Rev. B*, *73*, 235111.
[14] Duffy, J. A. (2006). *J. Phys. Chem. A*, *110*, 13245–13248.

[15] Waseda, Y., & Toguri, J. M. (1998). *The Structure and Properties of Oxide Melts: Application of Basic Science to Metallurgical Processing*, WSP: Singapore.
[16] Tanabe, S. (2015). *Int. J. Appl. Glass Sci.*, *6*, 305–328.
[17] Boetti, N. G. et al., (2013). *J. Non-Cryst. Solids*, *377*, 100–104.
[18] Suzuki, T. et al., (2010). *J. Non-Cryst. Solids*, *356*, 2344–2349.
[19] Harley, G., et al. (2009). *J. Non-Cryst. Solids*, *355*, 932–937.
[20] Quintas, A. et al., (2008). *J. Non-Cryst. Solids*, *354*, 98–104.
[21] Hoppe, U. et al., (2001). *Z. Naturforsch.*, *56a*, 237–243.
[22] Ropp, R. C. (2013). *Encyclopedia of the Alkaline Earth Compounds*, Elsevier: Amsterdam.
[23] Harley, G. A. (2008). *Proton transport in lanthanum phosphates*, Ph.D. dissertation, ProQuest LLC: Ann Arbor, USA.
[24] Fujino, S., & Kuwabara, M. (2006). *Key Eng. Mater.*, *320*, 209–212.